All-Electrochemical Synthesis of Submicrometer Cu Structures on Electrochemically Machined p-Si Substrates

Andrew L. Trimmer,[†] Joseph J. Maurer,[†] Rolf Schuster,[‡] Giovanni Zangari,[§] and John L. Hudson*,[†]

Department of Chemical Engineering, 102 Engineers' Way, University of Virginia, Charlottesville, Virginia 22904, Physical Chemistry, Technical University of Darmstadt, Petersenstrasse 20 D-64287 Darmstadt, Germany, and Department of Materials Science and Engineering and Center for Electrochemical Science and Engineering, University of Virginia, P.O. Box 400745, Charlottesville, Virginia 22904

Received June 6, 2005. Revised Manuscript Received August 26, 2005

A maskless all-electrochemical method for the deposition of micro- and nanoscale Cu structures on p-Si is reported. The first step involves the electrochemical machining of p-type Si in HF by applying nanosecond voltage pulses between a tool and a Si electrode. This process generates a localized defect structure, which is successively utilized to achieve selective metal electrodeposition. The resolution of the process is limited mainly by the tool dimensions and by the time constants involved in electrochemical machining, which lead to a limited spread of the defect region on the Si surface. Copper isolated islands with 500 nm diameter have been grown by electrodeposition, with high selectivity. This process has the potential to become a preferred technique for the placement and growth of submicrometer metal islands on semiconductor surfaces.

Introduction

The selective deposition of submicrometer metallic features on Si is a processing issue of great interest in the electronics industry as well as in the production of novel micro- and nanosystems integrated with Si electronics. Conventional methods to synthesize submicrometer structures exploit lithography and etching steps; however, lithographic processes require significant capital investment and are increasingly subject to low yields when dealing with deep submicrometer resolution. Alternative methods for the spatially selective synthesis of nanostructures are consequently sought.

Electrodeposition is an advantageous technique for selective deposition since metal reduction and film formation depend on the availability of electron or hole states at the substrate surface, at the correct energy levels. By modulating substrate properties such as surface chemistry, topography, or electronic density of states over the length scale of interest, selective deposition could be achieved directly, without the need of physical masks. Various methods have been already envisioned to achieve selective electrodeposition by such principles.[1−6]

A novel method that utilizes electrochemical processes to generate spatially confined defects—and thus new spatially confined electronic states—on Si surfaces is electrochemical machining (ECM) with ultrashort voltage pulses. The ECM method was first successfully demonstrated on various metal electrodes[7−11] and recently extended to p-Si.[12] ECM applies short voltage pulses, of the order of 100 ns or less, between a tool and a substrate electrode. Due to the applied potential field a current flows between the tool and substrate electrodes and an anodic reaction occurs at the substrate. The spread of the anodic reaction on the substrate increases with the duration of the voltage pulse. With the use of a dc potential the anodic reaction can spread over the entire electrode, while short voltage pulses improve the resolution of the anodic reaction by allowing the current to flow only through the shortest paths. The extent by which the anodic dissolution reaction spreads on the substrate surface thus depends on the tool size and on the *actual* duration of the voltage pulse, which is determined not only by the external power supply but also by the intrinsic rise and decay time of the externally imposed perturbation in the system considered. The duration of these transients can be approximately estimated through a time constant $\tau = RC$, where R is the equivalent resistance to the current flow between tool and substrate and C the

* Corresponding author. E-mail: Hudson@virginia.edu.
[†] Department of Chemical Engineering, University of Virginia.
[‡] Technical University of Darmstadt.
[§] Department of Materials Science and Engineering and Center for Electrochemical Science and Engineering, University of Virginia.

(1) Homma, T.; Kubo, N.; Osaka, T. *Electrochim. Acta* **2003**, *48*, 3115.
(2) Choi, J.; Chen, Z.; Singh, R. K. *J. Electrochem. Soc.* **2003**, *150*, C563.
(3) Schmuki, P.; Erickson, L. E. *Phys. Rev. Lett.* **2000**, *85*, 2985.
(4) Sasano, J.; Schmuki, P.; Sakka, T.; Ogata, Y. H. *Electrochem. Solid State Lett.* **2004**, *7*, G98.
(5) Scheck, C.; Liu, Y. K.; Evans, P.; Schad, R.; Bowers, A.; Zangari, G.; Williams, J. R.; Issacs-Smith, T. F. *Phys. Rev. B* **2004**, *69*, 35334.
(6) Scheck, C.; Evans, P.; Schad, R.; Zangari, G.; Sorba, L.; Biasol, G.; Heun, S. *Appl. Phys. Lett.* **2005**, *86*, 133108.
(7) Schuster, R.; Kirchner, V.; Allongue, P.; Ertl, G. *Science* **2000**, *289*, 98.
(8) Kock, M.; Kirchner, V.; Schuster, R. *Electrochim. Acta* **2003**, *48*, 3213.
(9) Cagnon, L.; Kirchner, V.; Kock, M.; Schuster, R.; Ertl, G.; Gmelin, W. T.; Kuck, H. *Z. Phys. Chem. (Muenchen)* **2003**, *217*, 299.
(10) Kirchner, V.; Cagnon, L.; Schuster, R.; Ertl, G. *Appl. Phys. Lett.* **2001**, *79*, 1721.
(11) Trimmer, A. L.; Kock, M.; Schuster, R.; Hudson, J. L. *Appl. Phys. Lett.* **2003**, *82*, 3327.
(12) Allongue, P.; Jiang, P.; Kirchner, V.; Trimmer, A. L.; Schuster, R. *J. Phys. Chem. B* **2004**, *108*, 14434.

10.1021/cm051208s CCC: $30.25
Published on Web 12/03/2005

total capacitance of the tool/electrolyte/substrate system. In metals the main contributions to the capacitance are the electrochemical double layer capacitances C_{DL} at the two interfaces, which can be estimated as $C_{DL} = 10\ \mu F/cm^2$. In contrast to metals on semiconductor substrates an additional contribution is the space charge layer capacitance, C_{SC}, within the semiconductor surface; the equivalent capacitance of the electrode interface for short pulse Si ECM is thus the series combination of C_{DL} and C_{SC}. The p-Si substrate electrode in this work is held at potentials where despite an anodic bias the p-Si is still in depletion.[13] C_{SC} of depleted p-Si can be calculated by the formula $C_{SC} = (q\epsilon_{Si}\epsilon_0 N_A/2)^{1/2}(V_B)^{-1/2}$,[14] where q is the electronic charge, ϵ_{Si} is the relative permittivity of Si, ϵ_0 is the permittivity of free space, N_A is the volume concentration of acceptor atoms, and V_B is the voltage due to the band bending inside the Si. For example, Si with a doping density of 9.9×10^{19} atoms/cm^3 (0.001 Ω·cm) has a space charge capacitance C_{SC} ($\epsilon_{Si} = 11.9$, $V_B = 0.5$ V) = 4 μF/cm^2, leading to an equivalent capacitance of 2.9 μF/cm^2. This would lead to a smaller time constant for the double layer charging as compared to metals and ultimately to a coarser resolution of the Si ECM. This is indeed observed in previously reported experiments: while a machining precision below 100 nm was achieved for nickel machining,[8] under similar machining conditions the achieved precision was more than 1 μm for highly doped p-Si.[12]

In this work we investigate the effect of the ultrashort pulse ECM experimental parameters on the dimensions and morphology of machined features on Si, with the objective to reproducibly generate submicrometer size defects. Electrodeposition of Cu on these features is further explored as an electrochemically simple model system to determine the conditions under which selective metal electrodeposition is achieved. We thus demonstrate the ability to selectively deposit Cu islands with 500 nm diameter, limited only by the dimensions of the defects that can be generated on Si.

Experimental Section

Si samples were cut from p-Si (100) wafers polished on a single side, with a resistivity of 0.001−0.002 Ω·cm (University Wafer). Tool electrodes were made from tungsten wires (99.99% Alfa Aesar) with a diameter of 100 μm. The wire diameter was tapered down to ∼200 nm at the wire tip via electrochemical etching in 1 M NaOH, using a method similar to that employed to make STM tips.[15] The tip shaft was covered in apiezon wax, reducing the tool area exposed only to the sharp end that was utilized for machining.

The electrochemical machining of the p-Si samples was conducted in a manner similar to that described in ref. 12. The experimental setup is described in detail in refs 7 and 8. The potentials of the tool, U_{tool}, and of the Si substrate, U_{Si}, were separately controlled using a custom-made bipotentiostat. A platinum wire served as the counter electrode, and a palladium wire loaded with hydrogen served as a quasi-reference electrode; potentials are here reported versus the Pd|H reference, which is +50 mV in the standard hydrogen scale.[16] High-frequency pulses were generated by a pulse generator (Agilent 81110A) and were delivered to the tool electrode via a custom-made amplifier that accounts for cell impedance. The pulses were applied to the tool electrode such that the "off" value corresponded to the reported tool potential U_{tool}. When the pulse was "on", the potential was lowered (in the cathodic direction) with respect to U_{tool} by the quantity reported as the pulse amplitude. Electrolytes of 1M HF were utilized for p-Si machining. The relevant machining conditions used to generate the features reported in this paper are listed in the corresponding figure captions.

Copper electrodeposition was performed after the machining process, in the same electrochemical cell and using the same counter and reference electrodes. Cu deposition was performed using electrolytes containing various concentrations of $CuSO_4$ with supporting HF or H_2SO_4. As was the case with the machining process, the precise experimental conditions utilized in the deposition process, including the electrolyte, are noted in the corresponding figure captions.

Scanning electron micrographs (SEM) and energy-dispersive X-ray spectroscopy data were collected using a JEOL 6700F microscope.

Results and Discussion

A p-Si/electrolyte interface under anodic polarization behaves similarly to a Schottky diode under forward bias. Scanning the applied potential anodically from the open circuit potential decreases the potential barrier for hole transport within the p-Si. Holes (h^+) can thus jump the barrier and be captured by surface bonds, initiating Si dissolution. Two dissolution paths are possible, as summarized in the following simplified reactions[17]

$$\mathrm{Si} + 2\mathrm{h}^+ \rightarrow \mathrm{Si}^{2+}$$
$$\mathrm{Si}^{2+} + 2\mathrm{H}^+ \rightarrow \mathrm{Si}^{4+} + \mathrm{H}_2 \quad (1)$$

and

$$\mathrm{Si} + 4\mathrm{h}^+ \rightarrow \mathrm{Si}^{4+} \quad (2)$$

The complex details of these reactions can be found in various published models.[17−20] Reaction 1 occurs in the potential region $U_{ocp} < U_{Si} < U_{peak}$, where U_{ocp} is the open circuit potential and U_{peak} is the potential at the first characteristic peak found in the anodic voltammogram of the Si/aqueous HF system. This region is characterized by low current densities and applied potentials. Reaction 1 consists of the direct dissolution of Si, and the second step occurs in solution with the evolution of hydrogen gas. Overall the process is divalent, and the result is porous Si formation. At potentials $U_{Si} > U_{peak}$ reaction 2 dominates. Reaction 2 is the indirect dissolution of Si, where a thin oxide is first formed at the interface, which is chemically removed via reaction with fluoride ions. Dissolution in this region is

(13) Ozanam, F.; Chazalviel, J. N. *J. Electron Spectrosc. Relat. Phenom.* **1993**, *64/65*, 395.
(14) Morrison, S. R. *Electrochemistry at Semiconductor and Oxidized Metal Electrodes*; Plenum Press: New York, 1980.
(15) Klein, M.; Schwitzgebel, G. *Rev. Sci. Instrum.* **1997**, *68*, 3099.
(16) Hoare, J. P.; Schuldiner, S. *J. Phys. Chem.* **1957**, *61*, 399.
(17) Zhang, X. G. *Electrochemistry of Silicon and Its Oxide*; Kluwer Academic/Plenum Publishers: New York, 2001.
(18) Searson, P. C. The Surface Chemistry of Silicon in Fluoride Electrolytes. In *Advances in Electrochemical Science and Engineering*; Gerischer, H., Tobias, C. W., Eds.; VCH: Weinheim, Germany, 1995; Vol. 4; p 67.
(19) Allongue, P.; Kieling, V.; Gerischer, H. *Electrochim. Acta* **1995**, *40*, 1353.
(20) Zhang, X. G. *J. Electrochem. Soc.* **2004**, *151*, C69.

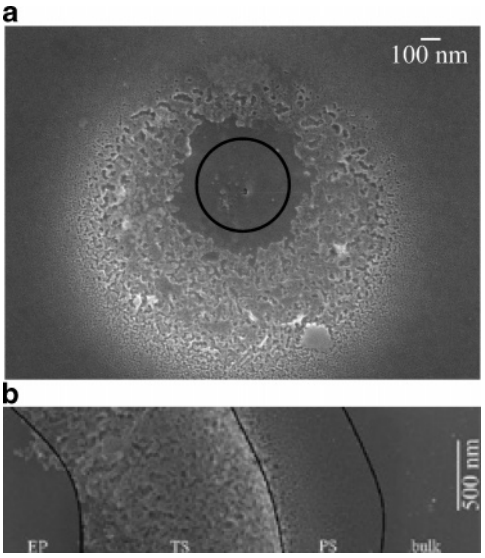

Figure 1. (a) Scanning electron micrograph of a machined p-Si feature; tool location is indicated by the outlined circle. Experimental conditions: $U_{Si} = -340$ mV, $U_{tool} = 10$ mV, 30 ns pulse duration, 1.3 V pulse amplitude, 0.5 μm penetration depth. (b) Magnification of the edge of a machined p-Si feature where electropolished (EP), transition (TS), porous (PS), and bulk regions are outlined. Experimental conditions: $U_{Si} = -250$ mV, $U_{tool} = 5$ mV, 30 ns pulse duration, 1.3 V amplitude, 1.5 μm penetration depth.

homogeneous, since the rate-limiting step is oxide dissolution, resulting in smooth surfaces. Hence, this region is known as the electropolishing region.

During the voltage pulse, the electrochemical micromachining process generates a spatially inhomogeneous distribution of the potential on the substrate region in front of the tool, with large anodic overpotentials directly in front of the tool and smaller overpotentials farther away. Electropolishing processes (reaction 2) would thus occur inside a region directly in front of the tool, while porous Si formation (reaction 1) would be observed in an annular region outside the former one. The spatial extension of these regions is in principle a function of the applied pulse amplitude, pulse duration, electrolyte composition, Si doping level, and position of the tool electrode with respect to the p-Si surface. If desired, the machined hole obtained after ultrashort pulse ECM could be increased in size by alkaline chemical etching, which selectively removes the porous region of a given feature.[12]

Converse to the experiments described in ref 12, in this work small diameter tool electrodes were used to generate smaller features in the submicrometer range, and the porous Si regions were not removed. Figure 1a shows an electrochemically machined p-Si surface obtained at very small tool/p-Si separations, on the order of 100 nm, and large anodic polarization. The black circle indicates the estimated position and diameter of the tool electrode tip. These machining conditions resulted in an extremely flat, electropolished region extending only approximately 100 nm farther than the tool diameter. The higher resistance current paths between the tool and more distant regions of the p-Si substrate result in a lower anodic surface polarization and the occurrence of different surface reactions. Figure 1b shows a magnified edge region of a feature obtained under similar conditions. In this case the tool was located on the left side of the figure and the closest region was electropolished. The right side of the image represents the unreacted bulk p-Si surface. Between the electropolished area and the unreacted bulk p-Si, at least two morphologically distinct regions can be discerned that were the result of progressively longer current paths and lower anodic polarization of the p-Si surface.

The morphology shown in Figure 1 is unique, since it represents porous Si exhibiting a gradient in pore diameter as a consequence of a potential gradient applied with submicrometer precision. Porous structures in Figure 1 had a pore diameter ranging from 5 to 50 nm, classifying the structures as mesoporous.[21,22] The pore diameter was smallest at the regions farthest from the influence of the tool, and increased moving toward the tool, corresponding to an increase in average current density, in good agreement with work by Lehmann et al.[22] The porous structures closer to the tool started to show morphologies that could be attributed to reaction 2, which further eroded the Si surface and created a transition region with blended properties between the electropolished and fully porous regions.

Adjustment of the tool height with respect to the substrate allows for direct control over surface morphology. Penetration of the tool inside the original p-Si surface generates localized etch pits, probably corresponding to protrusions at the tool tip. In addition, the porous region is pushed at a greater radial distance from the tool (not shown). Holding the tool at a height of about 500 nm above the surface instead results in a much lower anodic polarization of the Si surface, and only transition or fully porous Si structures were obtained (not shown).

The applied pulse amplitude at the tool electrode is another experimental variable significantly affecting the morphology of the p-Si surface. The amplitude of the applied pulse was experimentally optimized to provide a polarization at the substrate electrode such that reaction 2 dominated only the machined surface region directly below the tool electrode while beyond the tool edge, where the current density was lower, reaction 1 occurred. The applied pulse amplitude used to generate the morphology described above approximately polarized the substrate into the region of U_{peak}. Applied potentials much larger than U_{peak} spoil resolution since the region associated with reaction 2 on the p-Si surface became significantly larger than the footprint of the tool electrode. Polarizations below U_{peak} only formed porous Si.

Cu deposition onto the machined p-Si surfaces was performed in a three-electrode cell using the same counter and reference electrodes as the machining step. All deposition experiments were performed in the dark to avoid photogeneration of charge carriers that could spontaneously reduce Cu ions at the p-Si/electrolyte interface. With the exception of the electrodeposition experiments using HF as the supporting electrolyte, the experiments reported in the following paragraphs made use of a double-pulse potential technique.[23] The first pulse at high overpotential seeded metal nuclei on the surface. The second pulse, at lower overpotential, was

(21) Lehmann, V. *Electrochemistry of Silicon*; Wiley-VCH: Weinheim, Germany, 2002.
(22) Lehmann, V.; Stengl, R.; Luigart, A. *Mater. Sci. Eng., B* **2000**, *69*, 11.
(23) Ueda, M.; Dietz, H.; Anders, A.; Kneppe, H.; Meixner, A.; Plieth, W. *Electrochim. Acta* **2002**, *48*, 377.

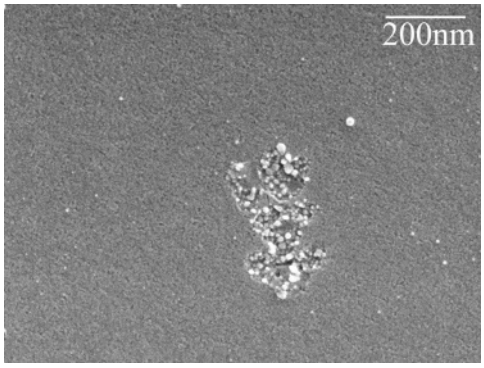

Figure 2. Scanning electron micrograph of electrodeposited Cu nuclei from a fluoride electrolyte on a machined p-Si structure. Machining conditions: $U_{Si} = -375$ mV, $U_{tool} = 10$ mV, 30 ns pulse duration, 1.7 V amplitude, tool penetrated into the surface. Cu deposition conditions: $U_{Si} = -650$ mV for 60 s in 16 μM $CuSO_4$ + 1 M HF in the dark.

used to grow existing nuclei without seeding new ones. In this way, initial seeds could be grown to form larger clusters without the parallel formation of new nuclei.

Theoretically, cathodic polarization of a p-Si/electrolyte interface is similar to a Schottky diode under reverse bias or current blocking conditions. Under these conditions, charge carriers reach the surface to participate in reduction processes only under two conditions: breakdown of the Schottky barrier at large applied external voltage, or photoexcitation of hole−electron pairs. The Cu deposition experiments were conducted in the dark, avoiding the latter possibility.

A study of Cu nucleation using an HF supported electrolyte was first undertaken. Figure 2 is a scanning electron micrograph of Cu deposition in a feature created via ultrashort pulse ECM. Cu nucleation density was greatest in the shallow depression in the center of Figure 2, which was created by the tool electrode, similar to the spot in the center of Figure 1a. The area surrounding the depression showed a much lower nucleation density and appeared roughened. Roughening of the Si surrounding the metal clusters has been previously reported and attributed to a spontaneous anodization of Si as a result of displacement by copper in fluoride electrolytes.[24,25] Cu was spontaneously reduced at random positions, including regions farther away from the tool, as confirmed by energy-dispersive X-ray spectroscopy performed on the same regions imaged by the SEM. Si roughening and Cu displacement occur at a much faster rate when using an HF supported electrolyte, thus only H_2SO_4 supported electrolytes were extensively studied in the following.

Figure 3 shows three scanning electron micrographs of a machined p-Si feature after potentiostatic seed and growth steps in a H_2SO_4 supported electrolyte. Before Cu deposition the p-Si feature looked much like that in Figure 1a. Parts a and b of Figure 3 represent the same area in the secondary electron and backscattered electron compositional imaging modes, respectively. The compositional mode clearly shows elemental contrast, with the Cu nuclei (higher atomic number) appearing as bright spots. The electropolished region surrounding the depression had a lower nucleation density than the center. Nucleation density increased on the transition region and significantly decreased on the outer porous band. The outer porous and the transition regions are shown in detail in Figure 3c.

The nuclei in the center of the ECM feature grew quickly, while other nuclei, especially those at the transition band, did not grow as fast or as large. The high growth rate in the center was probably due to the breakdown of the Schottky barrier facilitated by the presence of surface pits or other protruding defects. On the other hand, the transitional structures on the Si surface exhibit electronic properties intermediate between those of electropolished and mesoporous Si. Most notable among these properties is the lower conductivity of the porous regions due to charged surface traps constricting conduction paths in the porous skeleton by Coulombic repulsion.[26] In this transitional region, Cu nucleation was facilitated at pore bottoms, leading to a high nucleation density on wide pore bottoms or small areas of exposed Si. These nuclei however did not grow well, most likely due to a combination of lower conductivity of the surrounding porous structures and diffusional limitations of charge carriers at the pore base. It should be stressed here that the Cu clusters shown in Figure 3 and all electrodeposited features shown in the following figures passed the scotch tape test, demonstrating that there was considerable adhesion of the Cu features to the substrates.

Figure 3a shows a bright spot on the edge between the electropolished and the transition regions, which resulted from the initial tool contact with the surface prior to machining. A small portion of the W tool broke off and remained on the substrate, with the breakage confirmed by SEM inspection of the W tool post experimentation and the presence of the W confirmed by energy-dispersive X-ray spectroscopy during SEM imaging. This breakage happened occasionally during experiments, but did not cause any significant problems. In this example, the nucleation density was relatively high everywhere in Figure 3, and selectivity was low; conditions were thus sought to decrease the density of nuclei in regions farther away from the tool. One simple way to accomplish this was to reduce the duration of the potentiostatic pulse for nucleation.

Figure 4 is a scanning electron micrograph of a p-Si feature where less Cu was deposited as a result of short nucleation and growth times and slightly lower applied deposition potentials. Transition and porous bands were less visible in this case because the tool only moved into the p-Si approximately 100 nm. Cu nucleation density was greatest at the shallow pits directly under the tool electrode. During the second potentiostatic step the nuclei quickly grew together into the large single feature in the center of Figure 4. Smaller nuclei occurred sporadically on the regions that were not directly beneath the tool electrode during the machining.

Figure 5 is a scanning electron micrograph showing Cu clusters grown onto the p-Si area penetrated by the tool. The

(24) Gorostiza, P.; Diaz, R.; Kulandainathan, M. A.; Sanz, F.; Morante, J. R. *J. Electroanal. Chem.* **1999**, *469*, 48.
(25) Morinaga, H.; Suyama, M.; Ohmi, T. *J. Electrochem. Soc.* **1994**, *141*, 2834.
(26) Lehmann, V.; Hofmann, F.; Moller, F.; Gruning, U. *Thin Solid Films* **1995**, *255*, 20.

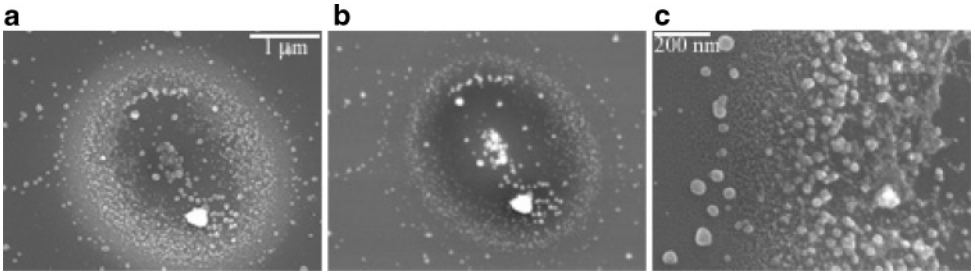

Figure 3. Scanning electron micrograph images of Cu deposition on a p-Si machined feature (a) region imaged in secondary electron mode, (b) backscattered electron image highlighting the metal deposits due to the atomic number contrast, and (c) secondary electron mode image of the edge wall area from (b). Machining conditions: $U_{Si} = -300$ mV, $U_{tool} = 10$ mV, 30 ns pulse duration, 1.7 V amplitude, tool penetrated into the surface. Deposition conditions: $U_{Si} = -650$ mV for 20 s in 16 μM $CuSO_4$ + 1 M H_2SO_4 followed by $U_{Si} = -350$ mV for 10 s in 1 mM $CuSO_4$ + 0.01 M H_2SO_4, in the dark.

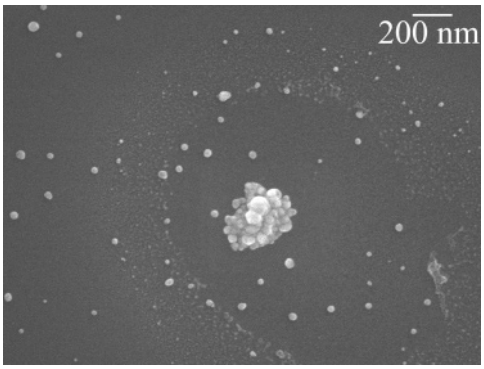

Figure 4. Scanning electron micrograph of Cu deposition on a machined p-Si sample with shorter deposition times. Machining conditions: $U_{Si} = -360$ mV, $U_{tool} = 10$ mV, 30 ns pulse duration, 1.7 V amplitude, tool penetrated into the surface. Deposition conditions: $U_{Si} = -600$ mV for 1 s in 16 μM $CuSO_4$ + 1 M H_2SO_4 followed by $U_{Si} = -250$ mV for 3 s in 1 mM $CuSO_4$ + 0.01 M H_2SO_4 in the dark.

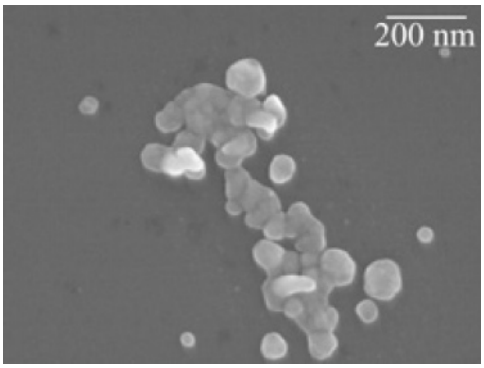

Figure 5. Scanning electron micrograph of a Cu cluster grown on a machined p-Si surface. Machining conditions: $U_{Si} = -330$ mV, $U_{tool} = 10$ mV, 10 ns pulse duration, 1.5 V amplitude, tool penetrated into the surface. Deposition conditions: $U_{Si} = -650$ mV for 25 s in 16 μM $CuSO_4$ + 1 M H_2SO_4 followed by $U_{Si} = -350$ mV for 15 s in 1 mM $CuSO_4$ + 0.01 M H_2SO_4 in the dark.

depth of the machined area was lower than the case shown in Figure 4; penetration was in fact limited to surface reliefs on the tool tip, thus the depth was probably on the order of 10 nm. Due to the shallow drilling depth and the ECM conditions used, the sample in Figure 5 did not show any clearly visible porous or transition region. Despite the weaker machining effect, the region directly beneath the tool still nucleated significant Cu compared that of to the bulk. Additionally, the region surrounding the Cu clusters remained smooth.

On the basis of the previous results shown in Figures 3−5, it is possible to rank the different features resulting from ECM according to their ability to favor Cu nucleation. With the application of an increasingly cathodic external potential, Cu will first nucleate on roughened electropolished regions resulting from the tool drilling into the surface, then on wide pore transition regions, then on flat electropolished regions, and finally on fully porous regions. Nucleation density was highest on the electropolished region below the tool where penetration of the p-Si surface occurred. The high nucleation density and fast growth rate in this instance were likely due to Schottky barrier breakdown, which was probably facilitated by the high density of surface defects as compared to intact, smooth surfaces. Schottky breakdown has been in fact demonstrated on p-Si where the defects were created with a nanoindenter[1] or an ion beam.[3] Nucleation on regions where only porous Si formed on the other hand was least likely since these structures had a lower conductivity compared to that of the bulk.[26] Nucleation density was high on transition structures but growth was slow since the electronic surface properties of the transition structure were between those of electropolished and porous Si. Where crystalline p-Si was exposed, at pore bottoms, the nucleation density was high, but the surrounding porous skeleton with low conductivity inhibited the growth.

Cu nucleation on the bulk, nonmachined areas of the p-Si surface is obviously undesirable if this method is to be used as a maskless process. Much of the bulk Cu deposition in the previous figures was thought to be a result of the long immersion times needed to complete the machining of arrays of these features. In these situations the p-Si was exposed to 1 M HF for periods ranging from 30 to 75 min. Longer machining times resulted in the slow chemical etching of bulk p-Si thus making it more susceptible to Cu deposition.

Figure 6 shows an experiment where the total HF exposure time was less than 30 min to minimize chemical etching of the bulk p-Si. In this case, images were taken before and after Cu deposition. Figure 6a is the image before plating, showing a roughened structure at the tool position but no significant transition or porous structures. Since the tool did not significantly penetrate the surface, no smooth electropolished region was observed. The morphology of this feature was due to the limited extent of tool penetration and the lower applied potential compared to the other cases. This combination of machining parameters, i.e., the reduced machining time, the limited tool penetration, and lower applied potential, formed surface regions that were highly attractive for selective Cu nucleation. Figure 6b shows a Cu island grown onto the feature in Figure 6a. The island is polycrystalline

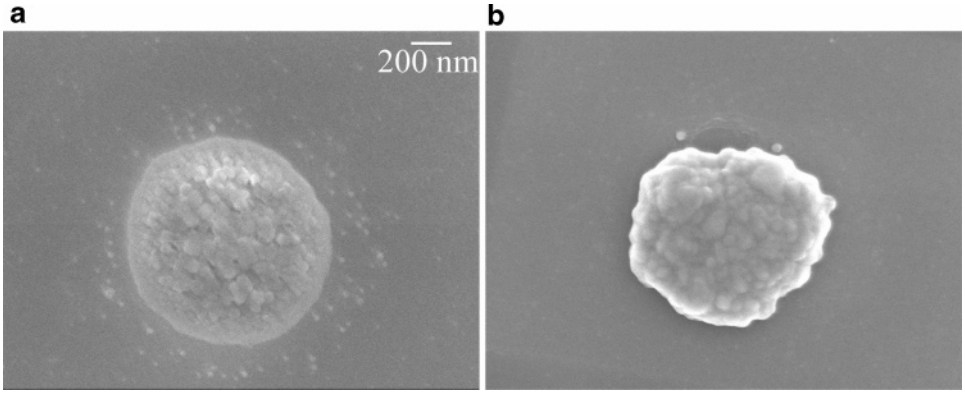

Figure 6. (a) Scanning electron micrograph of a p-Si roughened surface feature with an HF exposure of less than 30 min. Machining conditions: $U_{Si} = -290$ mV, $U_{tool} = 15$ mV, 30 ns pulse duration, 1.3 V amplitude, tool penetrated into the surface. (b) Cu island grown onto the feature shown in (a). Deposition conditions: $U_{Si} = -500$ mV for 10 s in 1 mM $CuSO_4$ + 0.01 M H_2SO_4 followed by $U_{Si} = -350$ mV for 10 s in 0.05 M $CuSO_4$ + 0.5 M H_2SO_4 in the dark.

but compact; it closely replicates the defect structure where selective nucleation occurs and does not seem generated by the coalescence of different nuclei. In addition, selectivity is very high; no other Cu nuclei were observed in regions away from the machined feature. This result thus demonstrates that the ultimate resolution of this process is determined by the tool size and by the ECM conditions; a decrease in the smallest feature of at least 1 order of magnitude should be possible by using tips with a smaller footprint.

Conclusions

Selective, maskless deposition of Cu features onto ultrashort pulse ECM submicrometer structures generated on p-Si was demonstrated. The machining process produced a range of morphologies on the surface that exhibit different nucleation overvoltages. Roughened electropolished regions, resulting from tool penetration into the surface, are the most active regions for Cu nucleation. High activity in these regions was likely due to Schottky barrier breakdown, which was facilitated by the presence of surface defects. Porous structures at the outer edge of the machined region nucleate the least Cu. Porous structures had different conductivity compared to that of the bulk due to charge carrier depletion, resulting in slower Cu growth. The ECM of p-Si using ultrashort voltage pulses followed by electrochemical deposition thus resulted in the fabrication of self-aligned Cu features of about 500 nm in size. Miniaturization is currently limited by the size of the machined feature, which in turn depends on the tip size of the tool employed. We believe that this entirely electrochemical method has the potential to become the technique of reference to achieve maskless, self-aligned deposition of Cu and other metals on Si.

Acknowledgment. This work was supported by the Center for Nanoscopic Materials Design, a National Science Foundation Materials Research Science and Engineering Center at the University of Virginia.

CM051208S